MECSOL 2022 - Proceedings of the 8th International Symposium on Solid Mechanics
M.L. Bittencourt, J. Labaki, L.C.M. Vieira Jr. and E. Mesquita (Editors), Campinas SP, Brazil, October 17th to 19th, 2022

Structural Health Monitoring of Thermoplastic Composite Beams via Vibration-based Method

P.B. Ataabadi[1], Denys Eduardo Teixeira Marques[2], Bruno Guilherme Christoff[2], Marcelo Leite Ribeiro[2], M. Alves[1], and Volnei Tita[2,3]

[1] University of Sao Paulo, Group of Solid Mechanics and Structural Impact, Department of Mechatronics and Mechanical Systems Engineering, Sao Paulo 05508900, Brazil

[2] University of Sao Paulo, Sao Carlos School of Engineering, Department of Aeronautical Engineering, Av. João Dagnone, 1100 - Jardim Santa Angelina, 13563-120, Sao Carlos (SP), Brazil

[3] Faculty of Engineering of University of Porto, Department of Mechanical Engineering, Rua Dr. Roberto Frias s/n, 4200-465, Porto, Portugal

Abstract: The present study aims to investigate the capability of new sensors to detect impact-induced damage in composite beams via VBM (Vibration-based Method). Laminated thermoplastic composite beams made of carbon fiber-reinforced polymer (CFRP) made of unidirectional layers are used as specimens in this investigation. Any deviation in vibrational parameters of beams such as mode shapes, natural frequencies, and more importantly frequency response functions (FRFs) by using damage metrics, before and after impact, will be considered as a criterion to identify damage and structural integrity degradation. Besides experimental procedure, numerical simulation of low-velocity impact and vibrational analyses of composite beams will be performed to evaluate the possible advantages/disadvantages of the computational procedure, as well as the potentialities and limitations of the new sensors to be used in SHM (Structural Health Monitoring) systems.

Keywords: Structural Health Monitoring, Vibration-based method, Damage detection, Damage metrics, FE simulation, Experimental procedure, Composite beam.

INTRODUCTION

Concerns with the environmental issues and increase in fuel prices have led car and aircraft producing companies to incorporate Fiber-reinforced polymer (FRP) composite materials into their products as desirable substitutions for heavy conventional metallic materials. FRP composites due to their high specific strength and stiffness ratios, besides other suitable mechanical properties such as excellent corrosion and fatigue resistance, have been extensively utilized in the aerospace and automotive industries. Since vehicle (automobile and airplane) structures are likely to experience impact during their lifetime, FRP composites are prone to develop barely visible impact damage (BVID) and visible damages. Thus, a wide range of periodic inspection schemes including simple visual inspection or advanced X-ray and ultrasonic methods is required to assure structural integrity. In many industries, especially in the aerospace industry, Structural Health Monitoring (SHM) systems have become more desired than the periodic inspection methods since the integrity status of the structure could be monitored continuously (online) and during service (Bergmayr, Kralovec, and Schagerl 2020). Thus, this continuous monitoring can increase structural safety and reduce expenses.

Several SHM systems like vibration-, optical-, thermal- and impedance-based methods have been used to detect damages (like impact-induced damages) (Loi, Porcu, and Aymerich 2021). Due to its simplicity, the vibration-based method has been widely developed by several researchers (Aymerich and Staszewski 2010; Medeiros et al. 2021; de Medeiros, Borges, and Tita 2014; de Medeiros, Vandepitte, and Tita 2018; Meo and Zumpano 2005; Zhou, Sun, and Huang 2019). Depending on the type of material and damage scenario, the presence of damage can lead to a change in stiffness, damping, mass, or geometry of the structure. This change leads to different dynamic responses from the equivalent intact structure. The vibration-based SHM method assesses the health condition of a specimen by considering dynamic responses(Cuadrado et al. 2022). In this method, vibrational responses of damaged and undamaged specimens, such as mode shapes, natural frequency, Frequency Response Functions (FRFs), and damping behavior, will be compared together.

The present research project aims to investigate the capability of new sensors to detect impact-induced damage in composite beams via VBM (Vibration-based Method). Since the new sensors are still being manufactured, at the present stage this conference paper only presents a similar procedure without using new sensors. Both experimental and numerical methods have been considered herein.

EXPERIMENTAL PROCEDURE

The experimental procedure has three stages; (I) vibration test on the intact beam, (II) lateral impact on the beam, and (III) vibration test on the damaged beam. The beam specimen in the present study is a unidirectional laminated composite with $[(0)_{14}]$ stacking sequence. The fibers are parallel to the beam length. The mechanical properties of CFRP material are listed in Tab. 1.

Table 1 – Mechanical properties of FRP composite.

Properties	Value	Properties	value
Elastic properties		Strength parameters	
E_{11} (GPa)	122.33	X^{T*} (MPa)	1404
E_{22} (GPa)	6.78	Y^{T*} (MPa)	21.55
G_{12} (GPa)	3.47	$S_{12}{}^{*}$ (MPa)	37.71
Major poison's ratio	0.287	$S_{21}{}^{*}$ (MPa)	-
		X^{C*} (MPa)	800**
		Y^{C*} (MPa)	200**

* X (1) represents fiber direction; Y (2) represents the direction transverse to the fibers; T stands for tensile and C stands for compressive properties; S stands for shear strength.

** The values are assumed.

The beam specimen was cut from a unidirectional laminated plate, as illustrated in Fig. 1. The position of the beam on the shaker (fixed boundary), impact area, and location of the measuring point are described in Fig. 1.

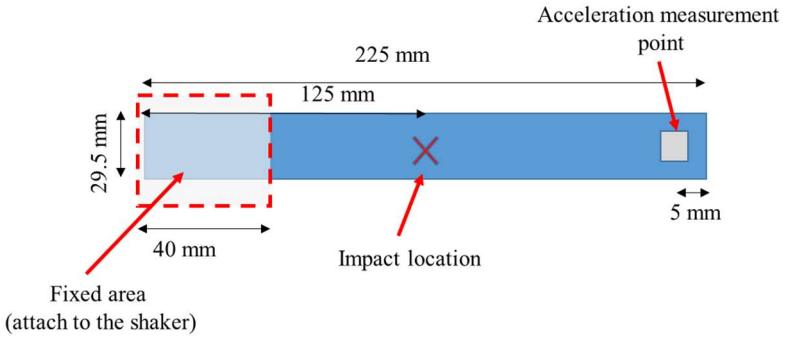

Figure 1- Beam specimens dimension, location of the impact point, cantilever boundary condition, and measurement point.

In the first stage the intact beam was attached to the shaker (cantilever beam) and a harmonic excitation with variable frequency (0 to 550) Hz was applied to the fixation area. A laser vibrometer was utilized to measure the vibrational response of the beam at one point close to the free end of the beam. The vibration test setup is illustrated in Fig. 2. The vibration response (voltage from the laser vibrometer) was acquired 3 times to assure the repeatability of the procedure.

In the second stage, after the vibration test on the undamaged beam, the beam was removed from the shaker and placed under a low-energy drop-hammer facility at the GMSIE laboratory. A fixture designed to hold the beam on the drop hammer anvil during an impact test. The impact setup is presented in Fig. 3. The fixture only covers 60 mm of the beam length to not compressed the sensor that will be attached to the beam. The laser vibrometer was used to record the velocity of the impactor for further calculation. The impactor has a round shape with a 5.4 mm radius and 6.21 kg weight. The impactor was dropped from different heights (50, 100 mm) above the same position on the beam to induce different levels of damage on the beam.

After performing each impact test on the beam, the damaged beam was placed on the shaker with the same configuration presented in the first stage. The vibration response of the damaged beam at the selected point was recorded to be compared to the vibration response of the intact beam.

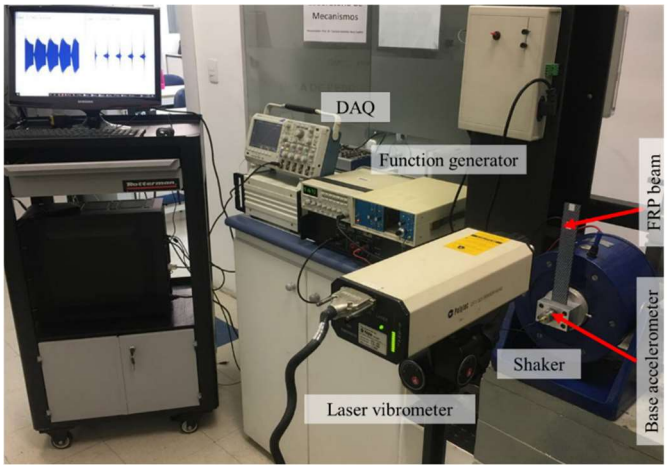

Figure 2- Vibration test setup.

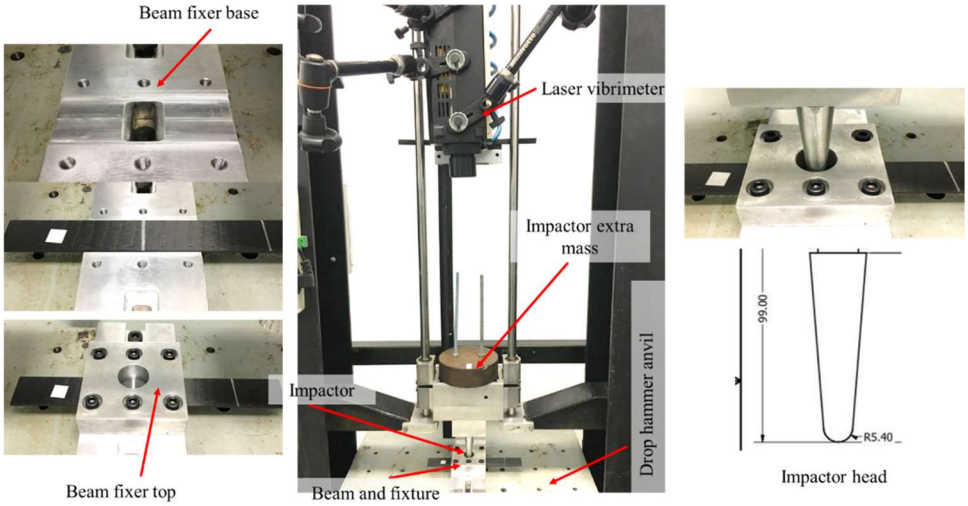

Figure 3 - Low-impact energy test setup.

Although the comparison between natural frequencies of intact and damaged structure is the simplest vibration-based structural health monitoring, this method may be more reliable when the damage extent is high. Thus, in the present work, besides comparing natural frequencies the damage metric will be used to detect damage on the beam. The damage qualifier presented by Mickens et al. (MICKENS et al. 2003) is used to quantify the difference in the FRF response (Fourier transform of the velocity of beam's tip divided by the Fourier transform of the acceleration of excitation of the shaker) between healthy and damaged structures. For discrete sampling data, Mickens damage index can be calculated from Eq. 1.

$$D = \frac{\Delta f}{f_2 - f_1} \sum_{i}^{n} y_i(f) \tag{1}$$

where f_1 and f_2 are the lower and upper frequency of the interest range, Δf is the frequency increment between acquired data and $y_i(f)$ is the percent difference between the magnitude of the FRFs of the intact and damaged beams.

$$y_i(f) = abs\left(\frac{|H^i| - |H^d|}{|H^i|}\right) \tag{2}$$

where $|H^i|$ and $|H^d|$ are FRFs of intact (superscript *i*) and damaged (superscript *d*) beams.

For a healthy structure damage index D is equal to zero, however, any increase in this index indicates that the structure is damaged.

NUMERICAL PROCEDURE

The numerical procedure similar to the experimental one has three stages; (I) modal analysis on the intact beam, (II) lateral impact on the beam, and (III) vibration test on the damaged beam.

The numerical simulations of experimental vibration and impact tests explained in the previous section were performed using ABAQUS 6.14. A multi-shell model of the composite beam was developed while the conventional shell element (S4R) was used to discretize the composite layers and interface layers were modeled with the continuum element. The composite shell layers were tied to the neighboring continuum cohesive layer by using the rigid tie. The global element size for all layers is equal to 1×1 mm. The FRP composite beam has $[(0)_{14}]$ layers however, to speed up the simulation this laminated was modeled with three layers of 0-direction laminate and two interface continuum layers $[(0)_5/C1/(0)_4/C2/(0)_5]$. The mechanical properties presented in Tab.1 were used as material input parameters. The material model uses Hashin's 2D failure criteria to detect the damage initiation of failure modes (mode I: Fiber tension, mode II: fiber compression, mode III: matrix tension, and mode IV: matrix compression). The fracture energies corresponding to each failure mode were assumed to be zero thus after damage initiation the mechanical properties of the failed element will be degraded to zero instantaneously. Figure 4 explains the FE model of the beam by presenting the FE model of impact simulation. The hard contact and tangential behavior with the penalty formula (0.35 friction coefficient) have been considered to act between all layers and surfaces in the FE model. The element-based cohesive model with traction-separation formula was used to represent the interface between composite layers. the mechanical properties of the cohesive layer were adopted from Ref. (Chiu et al. 2016) as listed in Tab. 2.

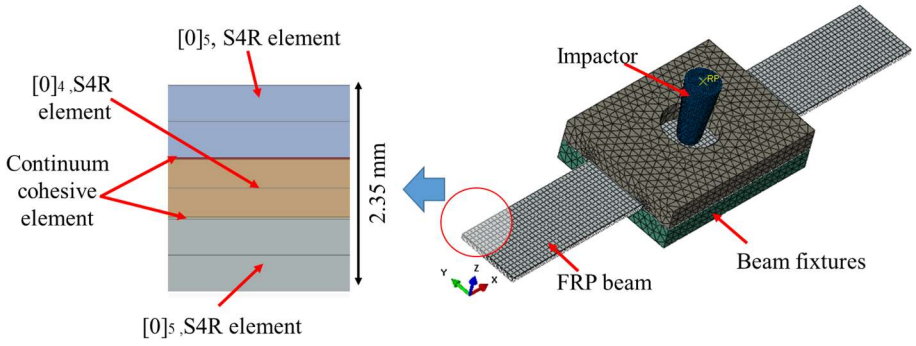

Figure 4 - FE model of impact simulation.

Table 2 – Mechanical properties of the interface layers (Chiu et al. 2016).

Failure mode	Interlaminar strenthes (MPa)	Interlaminar fracture energies (N/mm)
Mode I	$\sigma_I = 60$	0.331
Mode II	$\sigma_{II} = 60$	0.443

RESULTS

Figure 5 shows the comparison between the vibration response of intact and damaged beams in time and frequency domains. Based on the experimental vibration tests only the first natural frequency of the intact and damaged beams is noticeable in the FRF response of the beams. This issue could be related to the location measurement point on the beam.

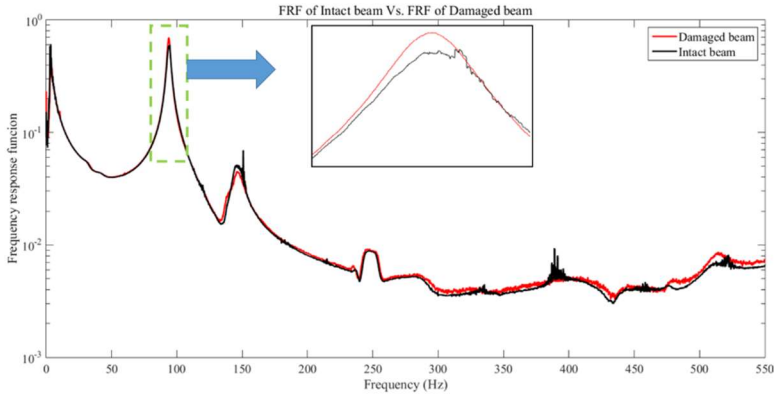

(a)

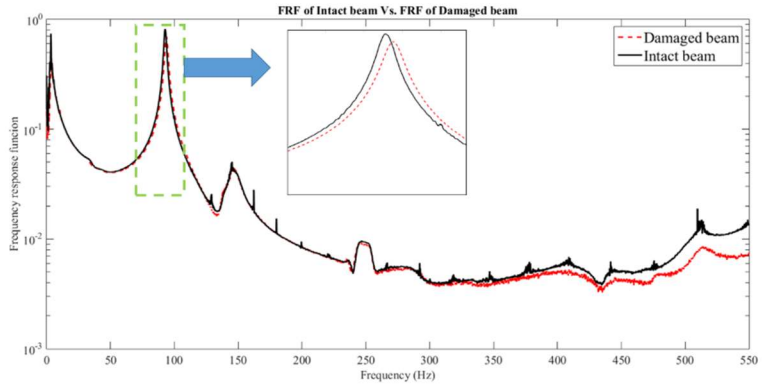

(b)

Figure 5 - Experimental FRFs of the tip of the beam for the intact and damaged; (a) Damage level I, (b) damage level II.

The values of damage indices calculated for the beam after the first and second impact are listed in Tab. 3. The increase in impact energy led to a higher level of damage, thus a 34 percent difference between the damage indices of the beam after the first and second impact was observed.

Table 3 - Damage Indexes for the FRP beam for different damage levels.

	Mickens damage index
Damage level I	0.0106
Damage level II	0.0161
Difference (%)	34.14

Figure 6 illustrates the damage to the beam after the impact tests. Based on the visual inspection the damage due to impact with the higher energy is more remarkable than the 3.1 J impact energy scenario, however, the invisible damages on the beam after the lower impact energy, like delamination, could be significant. The more reliable NDT test methods like the ultrasound test could be used to detect the damage extent.

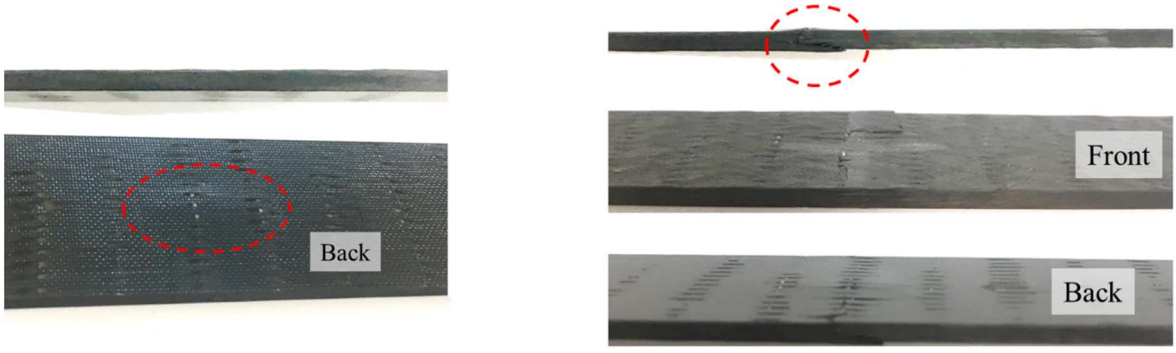

(a) (b)

Figure 6 – Visual damage level inspection; (a) Damage level due to the first impact with 3.1J energy, (b) Damage level due to the second impact with 4.34 J energy.

Figure 7 compares the impact force history of experimental and numerical simulation. There are some discrepancies between the experimental and numerical results. The main portion of this difference could be related to the assumption of interlaminar (composite ply) fracture energies and compressive strengths in the fiber and transverse to the fiber direction.

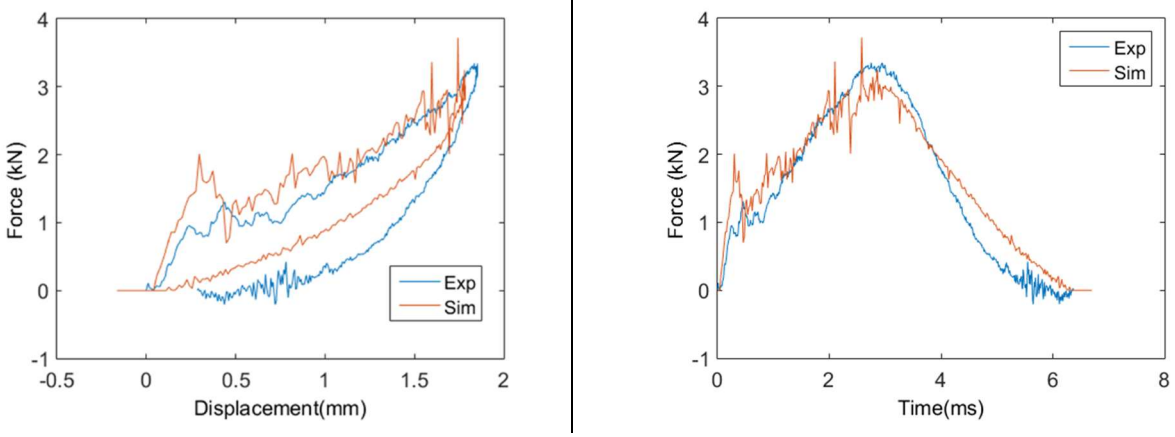

Figure 7- Comparison between impact force of experiment and simulation (3.10 J impact energy).

Figure 8 presents the different failure modes of composite plies (only L1, C1, and C2) for the end of the impact step. It is worth noting that the element deletion option for composite and cohesive layers has been turned off, thus totally failed elements were not deleted from the simulation.

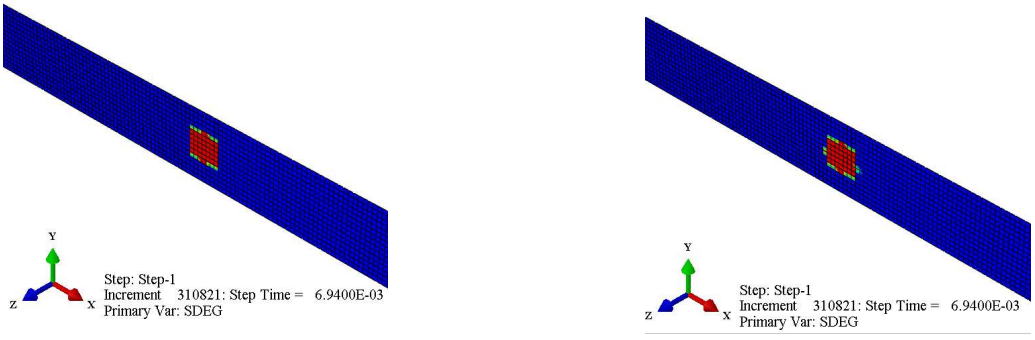

C1 C2

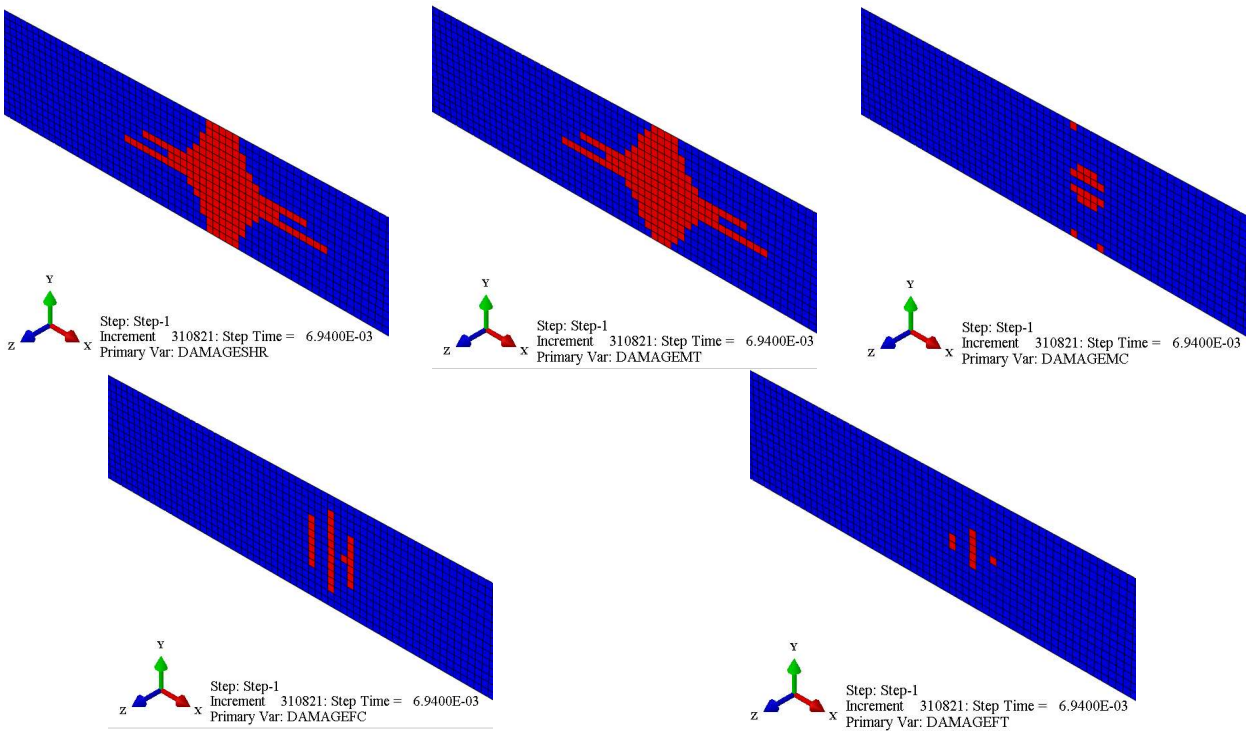

L1

Figure 8 - The damaged layer of the composite beam.

Abaqus/Standard was used to perform vibration analysis on the intact and damaged beams. The damaged model of the beam after impact (explicit simulation) was transferred to the ABAQUS Standard to compare the vibration behavior of intact and damaged models via FEA.

Modal analysis on the damaged and undamaged cantilever beams (with the same boundary condition of the beam in the experimental vibration test) was performed and natural frequencies and mode shapes are presented in Tab. 4 and Fig. 9 and 10. The difference between natural frequencies of some modes is significant. Moreover, in the experimental procedure, a small difference between the first natural frequencies of the intact and damaged beams was observed, however, a more significant difference between natural frequencies was obtained via the FE model. This issue could be related to the material model (assumed some of the mechanical properties).

Table 4 - Comparison between natural frequencies of intact and damaged beams (impact energy 3.10 J).

Beam model	Frequencies (Hz)					
	f_1	f_2	f_3	f_4	f_5	f_6
Intact beam (Exp)	93.88	Not obtained by experimental tests				
Damaged beam (Exp)	92.83					
	1.10					
	Difference (%) (1 – damaged/intact)×100					
Intact beam (Sim)	93.03	336.63	569.54	945.54	1100.01	1539.50
Damaged beam (Sim)	80.70	323.27	527.62	594.08	1138.30	1484.00
	13.20	3.70	7.38	37.21	3.45	3.57
	Difference (%) (1 – damaged/intact)×100					

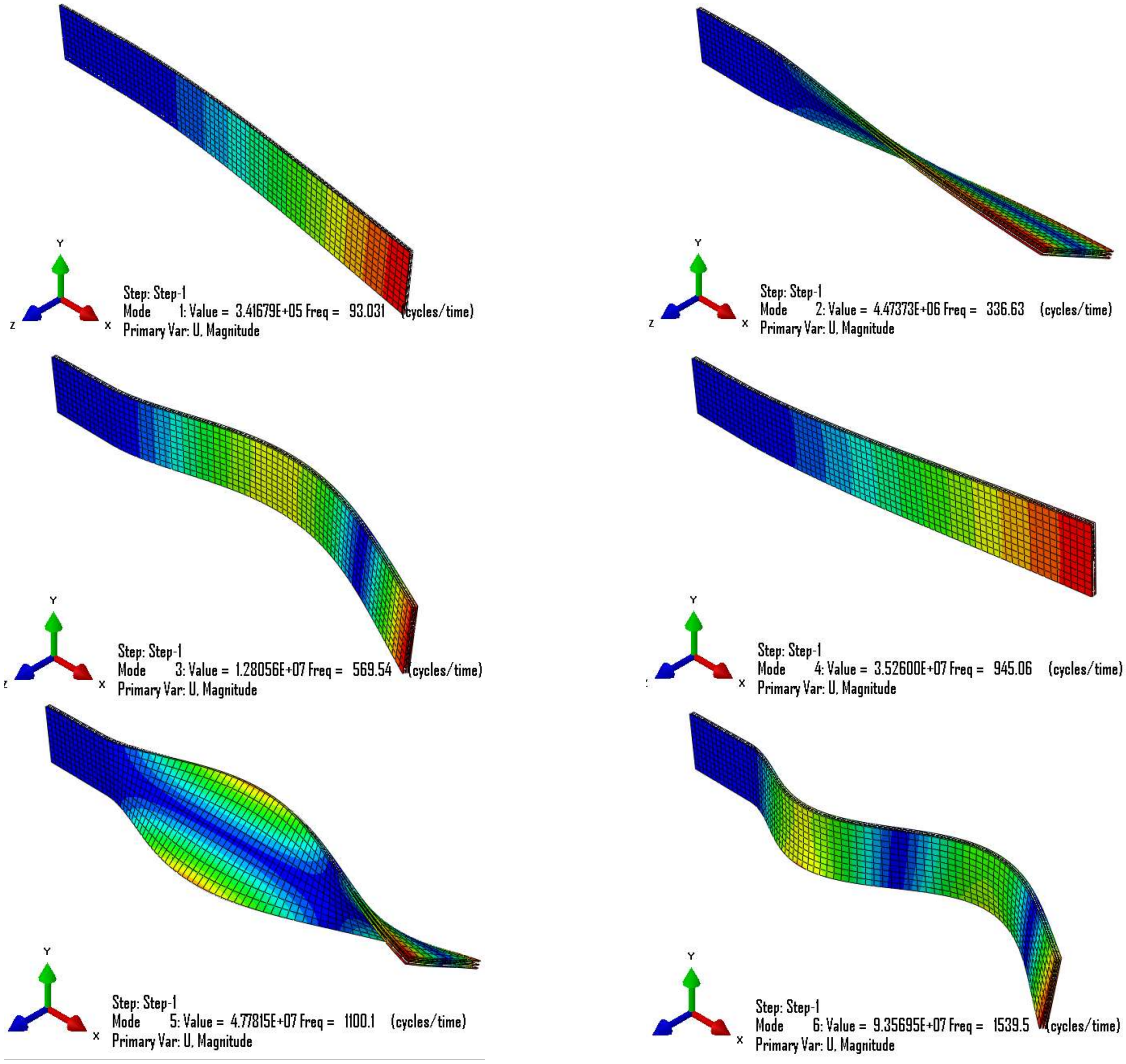

Figure 9 - Mode shapes of the intact beam.

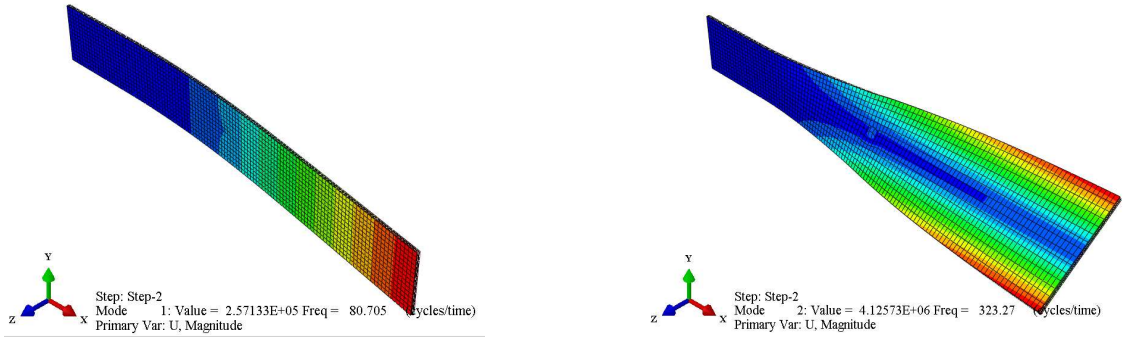

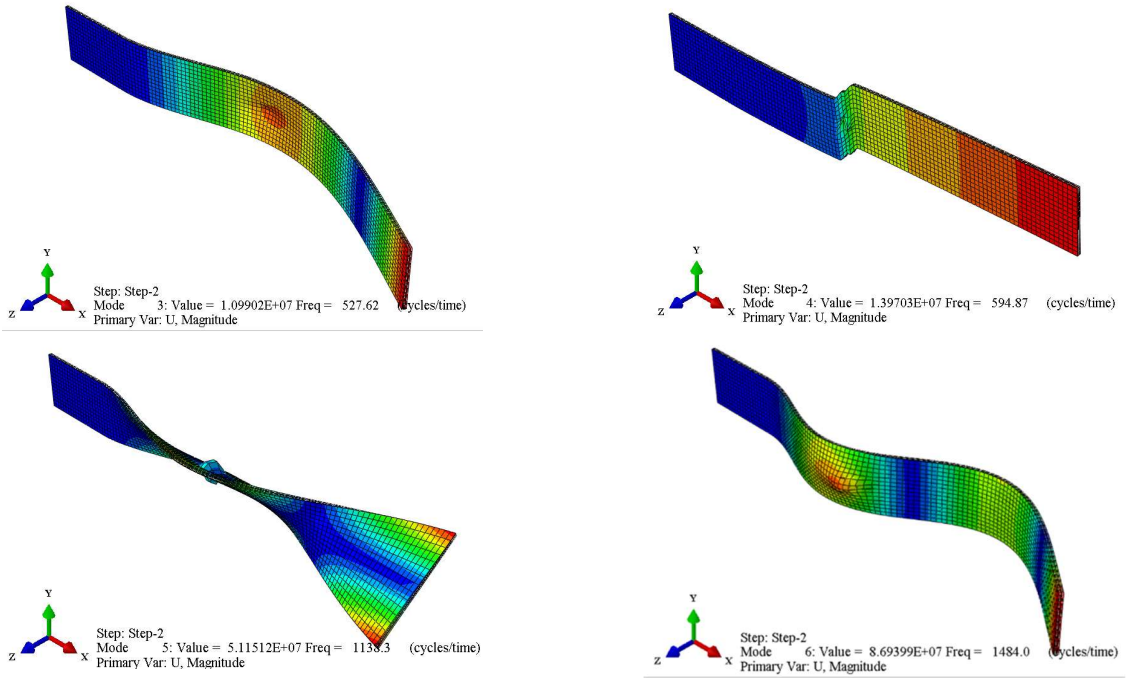

Figure 10 - Mode shapes of the damaged beam.

CONCLUSIONS

This work presents a numerical/experimental framework to detect the impact-induced damage to FRP composite materials through the correlation between the vibration response of intact and damaged beams. This framework will be utilized in the future to assess the damage detection capability of the new sensor that is going to be developed and tested in Portugal and Brazil.

ACKNOWLEDGMENTS

The authors are thankfull for the support of Dean's Office of Researcher of the University of Sao Paulo via "PIPAE - PROJETOS INTEGRADOS PARA PESQUISAS EM ÁREAS ESTRATÉGICAS". Volnei Tita would like to thank the National Council for Scientific and Technological Development (Conselho Nacional de Desenvolvimento Científico e Tecnológico; process number: 310656/2018-4).

REFERENCES

Aymerich, F. and W. J. Staszewski. 2010. "Impact Damage Detection in Composite Laminates Using Nonlinear Acoustics." *Composites Part A: Applied Science and Manufacturing* 41(9):1084–92.

Bergmayr, Thomas, Christoph Kralovec, and Martin Schagerl. 2020. "Vibration-Based Thermal Health Monitoring for Face Layer Debonding Detection in Aerospace Sandwich Structures." *Applied Sciences* 11(1):211.

Chiu, Louis N. S., Brian G. Falzon, Bernard Chen, and Wenyi Yan. 2016. "Validation of a 3D Damage Model for Predicting the Response of Composite Structures under Crushing Loads." *Composite Structures* 147:65–73.

Cuadrado, Manuel, Jesús Pernas-Sánchez, José Alfonso Artero-Guerrero, and David Varas. 2022. "Detection of Barely Visible Multi-Impact Damage on Carbon/Epoxy Composite Plates Using Frequency Response Function Correlation Analysis." *Measurement* 196:111194.

Loi, Gabriela, Maria Cristina Porcu, and Francesco Aymerich. 2021. "Impact Damage Detection in Composite Beams by Analysis of Non-Linearity under Pulse Excitation." *Journal of Composites Science* 5(2):39.

Medeiros, R., G. S. C. Souza, D. E. T. Marques, F. R. Flor, and V. Tita. 2021. "Vibration-Based Structural Monitoring of Bi-Clamped Metal-Composite Bonded Joint: Experimental and Numerical Analyses." *The Journal of Adhesion* 97(10):891–917.

de Medeiros, Ricardo, Emanuel Nunes Borges, and Volnei Tita. 2014. "Experimental Analyses of Metal-Composite Bonded Joints: Damage Identification." *Applied Adhesion Science* 2(1):13.

de Medeiros, Ricardo, Dirk Vandepitte, and Volnei Tita. 2018. "Structural Health Monitoring for Impact Damaged Composite: A New Methodology Based on a Combination of Techniques." *Structural Health Monitoring* 17(2):185–200.

Meo, M. and G. Zumpano. 2005. "Nonlinear Elastic Wave Spectroscopy Identification of Impact Damage on a Sandwich Plate." *Composite Structures* 71(3–4):469–74.

MICKENS, T., M. SCHULZ, M. SUNDARESAN, A. GHOSHAL, A. S. NASER, and R. REICHMEIDER. 2003. "STRUCTURAL HEALTH MONITORING OF AN AIRCRAFT JOINT." *Mechanical Systems and Signal Processing* 17(2):285–303.

Zhou, Yadong, Youchao Sun, and Tianlin Huang. 2019. "Bird-Strike Resistance of Composite Laminates with Different Materials." *Materials* 13(1):129.

RESPONSIBILITY NOTICE

The authors are the only parties responsible for the printed material included in this paper.